A comparison of glycine- and ivermectin-mediated conformational changes in the glycine receptor ligand-binding domain

Qian Wang and Joseph W. Lynch

Queensland Brain Institute and School of Biomedical Sciences, University of Queensland, Brisbane, QLD 4072, Australia.

Correspondence: Professor Joseph Lynch, Queensland Brain Institute, University of Queensland, Brisbane, QLD 4072, Australia. Tel. +617-3346-6375; Email: j.lynch@uq.edu.au

Keywords: ivermectin, Cys-loop receptor, gating, electrophysiology, voltage-clamp fluorometry.

Abstract

Glycine receptor chloride channels are Cys-loop receptor proteins that isomerize between a low affinity closed state and a high affinity ion-conducting state. There is currently much interest in understanding the mechanisms that link affinity changes with conductance changes. This essentially involves an agonist binding in the glycine receptor ligand-binding site initiating local conformational changes that propagate in a wave towards the channel gate. However, it has proved difficult to convincingly distinguish those agonist-induced domain movements that are critical for triggering activation from those that are simply local deformations to accommodate ligands in the site. We employed voltage-clamp fluorometry to compare conformational changes in the ligand-binding site in response to activation by glycine, which binds locally, and ivermectin, which binds in the transmembrane domain. We reasoned that ivermectin-mediated activation should initiate a conformational wave that propagates from the pore-lining domain towards the ligand-binding domain, eliciting conformational changes in those extracellular domains that are allosterically linked to the gate. We found that ivermectin indeed elicited conformational changes in ligand-binding domain loops C, D and F. This implies that conformational changes in these domains are important for activation. This result also provides a mechanism to explain how ivermectin potentiates glycine-induced channel activation.

1. Introduction

The glycine receptor (GlyR) chloride channel is a pentameric Cys-loop receptor that mediates fast inhibitory neurotransmission in the central nervous system (Lynch, 2009). Individual Cys-loop receptor subunits comprise a ligand-binding domain (LBD) and a transmembrane domain (TMD). The LBD consists of a 10-strand β-sandwich, comprising a six-strand inner β-sheet and a four-strand outer β-sheet (Brejc et al., 2001). Ligand-binding pockets, located at extracellular subunit interfaces, are lined by three loops (A, B and C) from the + side of the interface, and three β-strands (binding 'loops' D, E and F) from the - side. The TMD consists of a four α-helical bundle, with the second transmembrane (TM2) domains contributed by each of the five subunits lining a central water-filled pore. Cys-loop receptor channel activation involves structural rearrangements that originate at the ligand-binding site and propagate via the extracellular TM2-TM3 loops to the TM2 domains to create an open channel pore (Bocquet et al., 2009, Hilf and Dutzler, 2009, Miyazawa et al., 2003, Unwin, 2005, Zheng and Auerbach, 2011).

Agonist-binding induces loop C to 'clasp' around the bound agonist (Celie et al., 2005, Hansen et al., 2005, Mukhtasimova et al., 2005, Unwin et al., 2002, Venkatachalan and Czajkowski, 2008). Although molecular dynamics simulations predict that this movement triggers channel opening (Law et al., 2005), experimental support for this is lacking to date. Moreover, because agonists and antagonists both induce conformational changes in loops C and F, it remains a subject of debate as to whether these movements represent local deformations in response to ligand-binding or whether they also initiate channel activation (Khatri et al., 2009, Khatri and Weiss, 2010, Pless and Lynch, 2009, Wang et al., 2010, Zhang et al., 2009, Celie et al., 2005, Thompson et al., 2006). A new approach is needed to establish whether an allosteric link exists between these ligand-binding loops and the gate. We reasoned that if the pore can be induced to open without agonist occupation of the LBD ligand-binding site, then conformational changes initiated by the opening of the pore will propagate from the TM2 domains in reverse to the LBD, eliciting conformational changes in those domains that are allosterically linked to the pore gate.

Ivermectin is ideal for this purpose as it directly activates both the GlyR and the structurally-related glutamate-gated chloride channel receptor (GluClR) (Pless et al., 2007, Shan et al., 2001) and it has recently been shown to bind in a common TMD location in the GluClR (Hibbs and Gouaux, 2011) and the GlyR (Lynagh and Lynch, 2010a, Lynagh et al., 2011). Here we used voltage-clamp fluorometry (VCF) to compare glycine- and ivermectin-induced conformational changes at 12 fluorescently labeled sites throughout the GlyR LBD. VCF involves covalently labeling domains of interest with environmentally-sensitive fluorophores. Because changes in fluorophore quantum efficiency occur in response to alterations in their chemical environment, VCF reports local ligand-induced conformational changes occurring in real-time at receptor sites of interest (Gandhi and Isacoff, 2005, Pless and Lynch, 2008).

2. Materials and methods

2.1. Molecular biology

The rat α1 GlyR subunit cDNA was subcloned into the pGEMHE expression vector. The wild type (WT) and all mutant constructs incorporated the C41A mutation to eliminate the sole uncrosslinked extracellular cysteine. QuickChange (Stratagene, La Jolla, CA) was used to generate all cysteine mutants used in this study. The successful incorporation of the mutations was confirmed by the automated sequencing of the entire coding sequence. Capped mRNA for oocyte injection was generated using mMessage mMachine (Ambion, Austin, TX).

2.2. Reagents used in VCF experiments

Sulforhodamine methanethiosulfonate (MTS-R) and 2-((5(6)-tetramethylrhodamine) carboxylamino)ethyl methanethiosulfonate (MTS-TAMRA) were obtained from Toronto Research Chemicals (North York, ON). Alexa Fluor 546 C_5 maleimide (AF546) and tetramethylrhodamine-6-maleimide (TMRM) were from Invitrogen (Carlsbad, CA). MTS-R, MTS-TAMRA and TMRM were dissolved in dimethylsulfoxide and stored at -20°C. AF546 was dissolved directly into ND96 solution (96 mM NaCl, 2 mM KCl, 1 mM $MgCl_2$, 1.8 mM $CaCl_2$, 5 mM HEPES) on the day of the experiment. Ivermectin (Sigma-Aldrich) was stored at -20°C as a 100 mM stock in dimethylsulfoxide.

2.3. Oocyte preparation

Xenopus laevis oocytes (Xenopus Express, France) were prepared as previously described (Pless et al., 2007) and injected with 10 ng mRNA. They were then incubated at 18 °C for 3-5 days in a solution containing 96 mM NaCl, 2 mM KCl, 1 mM $MgCl_2$, 1.8 mM $CaCl_2$, 5 mM HEPES, 0.6 mM theophylline, 2.5 mM pyruvic acid, 50 µg/ml gentamycin, pH 7.4. On the day of recording, oocytes were transferred into ND96 containing a 10-20 µM concentration of fluorophore. Typical labeling times were 30 s for MTS-R and MTS-TAMRA, 30 min for TMRM and 45 min for AF546. Following labeling, oocytes were thoroughly washed in ND96 before use.

All fluorophores employed here respond with an increase in quantum efficiency as the hydrophobicity of their environment is increased (Chang and Weiss, 2002, Dahan et al., 2004). Each cysteine mutant was incubated with each of the four fluorophores in turn and generally the one yielding the largest glycine-induced fluorescence change (ΔF) was analysed. As unmutated GlyRs never exhibited a ΔF or a change in electrophysiological properties following fluorophore incubation, we rule out the possibility of labels binding nonspecifically to receptors.

2.4. VCF and Data Analysis

The experimental set up comprised an inverted fluorescence microscope (IX51, Olympus, Tokyo, Japan) equipped with a high-Q tetramethylrhodamine isothiocyanate filter set (Chroma Technology, Rockingham, VT), a LUCPlanFLN 40x/NA0.6 objective (Olympus), and a Hamamatsu H7360-03 photomultiplier (Hamamatsu Photonics, Iwata City, Japan) with a 12 V/100 W halogen lamp (Olympus) as light source. The recording chamber is similar to those described previously (35,36) (Dahan et al., 2004, Pless et al., 2007). Cells were voltage-clamped at -40 mV and currents were recorded with an OC-725C oocyte amplifier (Warner, Hamden, CT). Current and fluorescence traces were acquired at 200 Hz via a Digidata 1322A interface using pClamp 9.2 software (Axon Instruments, Union City, CA). Fluorescence signals were digitally filtered at 1-2 Hz with an eight-pole Bessel filter for analysis and display. Half-maximal concentrations (EC_{50}) and Hill coefficient (n_H) values for ligand-induced activation of current and fluorescence were obtained using the Hill equation, fitted with a non-linear least squares algorithm (SigmaPlot 9.0, Systat Software, Point Richmond, CA). All results are expressed as mean ± S.E.M. of three or more independent experiments. Unless otherwise indicated, statistical analysis was performed using unpaired Student's t-test, with $p < 0.05$ representing significance.

3. Results

We previously identified several extracellular sites that, when covalently labeled with environmentally-sensitive fluorophores, elicit robust glycine-induced ΔF responses (Pless et al., 2007, Pless and Lynch, 2009). Here we compared the peak magnitudes of glycine- and ivermectin-induced ΔFs of GlyRs incorporating labels at each of these positions, with and without a mutation (A288G) that enhances ivermectin sensitivity by 100-fold (Lynagh and Lynch, 2010b, Lynagh and Lynch, 2010a) or a double mutation (A288G-L233W) that converts ivermectin into an inhibitor of glycine-gated currents (Lynagh et al., 2011).

The following mutations were investigated: H201C and N203C in loop C, Q67C in loop D, S121C and L127C in loop E, V178C, A179C and G181C in loop F, E217C, Q219C and G221C in the pre-M1 domain and A52C in the β1−β2 loop. Following labeling as previously described (Pless and Lynch, 2009), the A52C, S121C, L127C, A179C, G181C, H201C, E217C, Q219C and G221C mutant GlyRs each exhibited robust ΔFs in response to glycine but exhibited no ΔF response to a saturating (30 μM) concentration of ivermectin (n = 5 - 10 oocytes each). Fig. 1A-C displays sample recordings from MTS-TAMRA-labeled A52C GlyRs, MTS-TAMRA-labeled H201C GlyRs and TMRM-labeled E217C GlyRs demonstrating the presence of robust glycine-mediated ΔF responses and the absence of ivermectin-mediated ΔF responses.

In contrast, GlyRs labeled at the Q67C, V178C or N203C positions each produced robust ΔFs in response to both glycine and ivermectin. The experimental approach applied to all three mutants is illustrated in Fig. 2. The glycine ΔI EC_{50}, n_H and ΔI_{max} values for unlabeled and MTS-TAMRA-labeled Q67C-A288G GlyRs are summarised in Table 1. Corresponding values for the MTS-TAMRA-labeled Q67C GlyR have previously been published (Pless and Lynch, 2009). We were unable to maintain electrophysiological recordings from triple mutant GlyRs for long enough to generate full concentration-response relationships. We suspect this was due to their high glycine-sensitivity. Due to the unavoidably high glycine concentration of the media, this would lead to a significant resting chloride flux that may have degraded the viability of the oocytes.

A saturating (3 mM) glycine concentration produced much larger ΔI_{max} and ΔF_{max} values than those elicited by a saturating (30 μM) concentration of ivermectin applied 3 min later (Fig. 2A). This was not due to incomplete recovery from slow desensitization as glycine responses recovered fully within one minute (not shown). A second glycine application applied 3 min after ivermectin also elicited reduced ΔI_{max} and ΔF_{max} values, probably due to desensitization or residual channel activity resulting from the slowly-reversible ivermectin activation. The labeled Q67C-A288G GlyR displayed a similar pattern of activity (Fig. 2B), with the major difference being that ivermectin exhibited faster channel opening, a proportionately larger ΔF_{max} and stronger

desensitization. These effects are expected given that A288G dramatically enhances ivermectin sensitivity (Lynagh and Lynch, 2010b, Lynagh and Lynch, 2010a). At the Q67C-A288G-L233W GlyR, ivermectin activated no detectable ΔI but elicited a robust ΔF_{max} (Fig. 2C). The mean ΔI_{max} and ΔF_{max} values for all three Q67C-containing GlyRs are presented in Fig. 3A-C. For each mutant, the ΔI_{max} and ΔF_{max} values activated by the first glycine application are normalized to one and these normalization factors are applied to the respective values induced by ivermectin and the second glycine application. It is notable that the ivermectin-mediated ΔI_{max} and ΔF_{max} values are both significantly smaller than those induced by the first glycine application for all three mutants. Note, however, that the Q67C and Q67C-A288G mutants elicit proportionately very different ΔF_{max} responses relative to ΔI_{max} magnitudes, tentatively suggesting that glycine and ivermectin may induce different conformational changes. However, it is also evident that ivermectin induces different desensitization rates in these two mutants and that glycine and ivermectin generally induce distinct desensitization rates at the same mutant. Due to the differing desensitization rates and the difficulty in applying agonist solutions rapidly to voltage-clamped oocytes, it is not possible to quantitatively compare ivermectin- and glycine-induced ΔI_{max} and ΔF_{max} values, and hence to draw inferences concerning possible differences in the conformational changes induced by these agonists. Nevertheless, Fig. 3 demonstrates that ivermectin induces detectable conformational changes in the vicinity of LBD loop D in both low and high ivermectin affinity GlyRs and in a mutant GlyR where ivermectin exhibits only antagonist activity.

Fig. 4A-C shows representative recordings from similar experiments performed on the AF546-labeled V178C GlyR, the V178C-A288G GlyR and the V178C-A288G-L233W GlyR, respectively. Fig. 5A-C summarises the results from these experiments averaged from 3-5 cells each and normalised as described above for Fig. 3. Notable differences relative to results presented in Fig. 3A-C include the second glycine-activated ΔI_{max} being significantly larger than the first glycine-activated ΔI_{max} in the labeled V178C GlyR (Fig. 4A, 5A) and the smaller magnitude of the second glycine-activated ΔF_{max} at all three AF546-labeled V178C mutant constructs (Fig. 5A-C). There is no evidence for ivermectin mediating different ΔF_{max} responses in the three constructs.

Finally, Fig. 6A-C shows examples of results of similar experimental protocols applied to the MTS-TAMRA-labeled N203C GlyR, the N203C-A288G GlyR and the N203C-A288G-L233W GlyR, respectively. Fig. 7A-C shows averaged results from these experiments averaged from 3-5 cells each and normalised as described above for Fig. 3. The results are generally consistent with those presented in Fig. 3.

4. Discussion

A ligand-induced ΔF implies that the fluorophore microenvironment has been altered by a direct fluorophore-ligand interaction, a ligand-induced local conformational change, a ligand-induced conformational change that propagates to the gate, or any combination of these effects (Pless and Lynch, 2009, Wang et al., 2010). A standard assumption that we have employed in this study is that if two ligands produce significantly different ΔF_{max} values then they report different local conformational changes (Khatri et al., 2009, Pless and Lynch, 2009, Wang et al., 2010, Muroi et al., 2009). However, the relative magnitudes of ΔF_{max} signals are not necessarily directly proportional to the magnitude of the conformational changes that produced them. Previous VCF studies on the α1 GlyR showed that an antagonist (strychnine) and an agonist (glycine) produced ΔF_{max} values of identical magnitude at most labeled sites in loops C and F (Pless and Lynch, 2009). The most conservative interpretation of these results is that both ligands produced an identical conformational change. Given that loops C and F are located close to the ligand-binding site, it is entirely feasible that a common conformational change may have resulted from a local ligand-induced distension that does not propagate to the gate. However, it is also possible that glycine and strychnine induced different conformational changes with the same ΔF_{max} at these same sites, with only the glycine-induced conformational change being transmitted to the gate. However, it has proved difficult to demonstrate this. Consequently, in the present study we adopted a new approach to investigate the existence of a direct allosteric linkage between the TMD and the agonist-binding loops.

The main finding of this study is that ivermectin induced conformational changes in the vicinity of V178C in loop F, N203C in loop C and D67C in loop D. Because ivermectin binds in the TMD to open the pore (Hibbs and Gouaux, 2011, Lynagh et al., 2011) and loops C, F and D lie in the outer and inner β-sheets of the LBD, respectively, it is evident that ivermectin induces a global receptor conformational change. The principle of reciprocity, which applies to all currently proposed mechanisms of agonist action, states simply that if binding affects activation, then activation must affect binding (Colquhoun, 1998, Colquhoun and Farrant, 1993). Thus, if the pore helices can be moved in a manner to simulate channel activation, this must elicit a conformational change that back-propagates to the glycine-binding site to induce conformational changes in those LBD domains that are essential for activation and for controlling glycine affinity. In accordance with this theory, ivermectin-binding indeed induced a reverse conformational wave that elicited conformational changes in loops C, D and F of the glycine-binding site. This implies an allosteric linkage between these domains and the TM2, suggesting in turn that agonist-induced conformational changes in loops C, D and F may be important for triggering activation.

In addition to these results, several labeled sites including A52C, S121C, L127C, G181C, H201C, E217C, Q219C and G221C showed detectable ΔF responses to glycine but not to ivermectin, indicating that ivermectin and glycine induce distinct conformational changes in the LBD. This is not surprising given that glycine and ivermectin bind in different locations and activate the GlyR via structurally distinct mechanisms (Hibbs and Gouaux, 2011, Pless and Lynch, 2009, Shan et al., 2001). It is therefore likely that the conformational changes induced in the agonist-binding loops by ivermectin are not identical to the glycine-mediated movements that trigger activation. Nevertheless, the results demonstrate an allosteric coupling between the pore-lining α-helices and the glycine-binding loops C, F and D.

We also found that ivermectin inhibition of the A288G-L233W GlyR is accompanied by conformational changes in the same three ligand-binding loops. This implies that ivermectin inhibition is also mediated by a global allosteric conformational change that inhibits rather than activates the receptor. We speculate that the L233W mutation alters TM2 conformation so that

ivermectin closes rather than opens the channel, even though the conformational changes ivermectin produces in the LBD may be similar to those associated with opening.

Finally, these results also provide a mechanistic basis for understanding how ivermectin potentiates glycine-gated currents (Shan et al., 2001) and permits glutamate to bind to the structurally-related GluClR (Hibbs and Gouaux, 2011). By altering binding conformation of domains lining the agonist-binding site, ivermectin may either facilitate agonist (glycine or glutamate) binding or facilitate agonist-induced conformational changes associated with channel activation.

Acknowledgements

This research was supported by the Australian Research Council and the National Health and Medical Research Council.

Abbreviations

AF546, Alexa Fluor 546 C_5 maleimide; GlyR, glycine receptor; LBD, ligand-binding domain; MTS-R, sulforhodamine methanethiosulfonate; MTS-TAMRA, 2-((5(6)-tetramethylrhodamine) carboxylamino)ethyl methanethiosulfonate; TMD, transmembrane domain; TMRM, tetramethylrhodamine-6-maleimide; VCF, voltage-clamp fluorometry.

References

Bocquet N, Nury H, Baaden M, Le Poupon C, Changeux JP, Delarue M, et al. X-ray structure of a pentameric ligand-gated ion channel in an apparently open conformation. Nature 2009;457:111-114.

Brejc K, van Dijk WJ, Klaassen RV, Schuurmans M, van Der Oost J, Smit AB, et al. Crystal structure of an ACh-binding protein reveals the ligand-binding domain of nicotinic receptors. Nature 2001;411:269-276.

Celie PH, Kasheverov IE, Mordvintsev DY, Hogg RC, van Nierop P, van Elk R, et al. Crystal structure of nicotinic acetylcholine receptor homolog AChBP in complex with an alpha-conotoxin PnIA variant. Nat Struct Mol Biol 2005;12:582-588.

Chang Y, Weiss DS. Site-specific fluorescence reveals distinct structural changes with GABA receptor activation and antagonism. Nat Neurosci 2002;5:1163-1168.
Colquhoun D. Binding, gating, affinity and efficacy: the interpretation of structure-activity relationships for agonists and of the effects of mutating receptors. Br J Pharmacol 1998;125:924-947.
Colquhoun D, Farrant M. Molecular pharmacology. The binding issue. Nature 1993;366:510-511.
Dahan DS, Dibas MI, Petersson EJ, Auyeung VC, Chanda B, Bezanilla F, et al. A fluorophore attached to nicotinic acetylcholine receptor beta M2 detects productive binding of agonist to the alpha delta site. Proc Natl Acad Sci U S A 2004;101:10195-10200.
Gandhi CS, Isacoff EY. Shedding light on membrane proteins. Trends Neurosci 2005;28:472-479.
Hansen SB, Sulzenbacher G, Huxford T, Marchot P, Taylor P, Bourne Y. Structures of Aplysia AChBP complexes with nicotinic agonists and antagonists reveal distinctive binding interfaces and conformations. Embo J 2005;24:3635-3646.
Hibbs RE, Gouaux E. Principles of activation and permeation in an anion-selective Cys-loop receptor. Nature 2011;474:54-60.
Hilf RJ, Dutzler R. Structure of a potentially open state of a proton-activated pentameric ligand-gated ion channel. Nature 2009;457:115-118.
Khatri A, Sedelnikova A, Weiss DS. Structural Rearrangements in Loop F of the GABA Receptor Signal Ligand Binding, Not Channel Activation. Biophys J 2009;96:45-55.
Khatri A, Weiss DS. The role of Loop F in the activation of the GABA receptor. J Physiol 2010;588:59-66.
Law RJ, Henchman RH, McCammon JA. A gating mechanism proposed from a simulation of a human alpha7 nicotinic acetylcholine receptor. Proc Natl Acad Sci U S A 2005;102:6813-6818.
Lynagh T, Lynch JW. A glycine residue essential for high ivermectin sensitivity in Cys-loop ion channel receptors. Int J Parasitol 2010a;40:1477-1481.
Lynagh T, Lynch JW. An improved ivermectin-activated chloride channel receptor for inhibiting electrical activity in defined neuronal populations. J Biol Chem 2010b;285:14890-14897.
Lynagh T, Webb TI, Dixon CL, Cromer BA, Lynch JW. Molecular determinants of ivermectin sensitivity at the glycine receptor chloride channel. J Biol Chem 2011;in press.
Lynch JW. Native glycine receptor subtypes and their physiological roles. Neuropharmacology 2009;56:303-309.
Miyazawa A, Fujiyoshi Y, Unwin N. Structure and gating mechanism of the acetylcholine receptor pore. Nature 2003;423:949-955.
Mukhtasimova N, Free C, Sine SM. Initial coupling of binding to gating mediated by conserved residues in the muscle nicotinic receptor. J Gen Physiol 2005;126:23-39.
Muroi Y, Theusch CM, Czajkowski C, Jackson MB. Distinct structural changes in the GABAA receptor elicited by pentobarbital and GABA. Biophys J 2009;96:499-509.
Pless SA, Dibas MI, Lester HA, Lynch JW. Conformational variability of the glycine receptor M2 domain in response to activation by different agonists. J Biol Chem 2007;282:36057-36067.
Pless SA, Lynch JW. Illuminating the structure and function of Cys-loop receptors. Clin Exp Pharmacol Physiol 2008;35:1137-1142.
Pless SA, Lynch JW. Ligand-specific conformational changes in the alpha 1 glycine receptor ligand-binding domain. J Biol Chem 2009;284:15847-15856.
Shan Q, Haddrill JL, Lynch JW. Ivermectin, an unconventional agonist of the glycine receptor chloride channel. J Biol Chem 2001;276:12556-12564.
Thompson AJ, Padgett CL, Lummis SC. Mutagenesis and molecular modeling reveal the importance of the 5-HT3 receptor F-loop. J Biol Chem 2006;281:16576-16582.
Unwin N. Refined structure of the nicotinic acetylcholine receptor at 4A resolution. J Mol Biol 2005;346:967-989.
Unwin N, Miyazawa A, Li J, Fujiyoshi Y. Activation of the nicotinic acetylcholine receptor involves a switch in conformation of the alpha subunits. J Mol Biol 2002;319:1165-1176.
Venkatachalan SP, Czajkowski C. A conserved salt bridge critical for GABA(A) receptor function and loop C dynamics. Proc Natl Acad Sci U S A 2008;105:13604-13609.

Wang Q, Pless SA, Lynch JW. Ligand- and subunit-specific conformational changes in the ligand-binding domain and the TM2-TM3 linker of {alpha}1 {beta}2 {gamma}2 GABAA receptors. J Biol Chem 2010;285:40373-40386.
Zhang J, Xue F, Chang Y. Agonist- and antagonist-induced conformational changes of loop F and their contributions to the rho1 GABA receptor function. J Physiol 2009;587:139-153.
Zheng W, Auerbach A. Decrypting the sequence of structural events during the gating transition of pentameric ligand-gated ion channels based on an interpolated elastic network model. PLoS Comput Biol 2011;7:e1001046.

Table Legend

Table 1. **Summary of results for glycine-activated current and fluorescence responses.**

Electrophysiological and fluorescence results are shown in normal and bold type, respectively.

Figure Legends

Fig. 1. **Examples of labeled mutant GlyRs exhibiting glycine- but not ivermectin-mediated ΔF responses.**

In this and subsequent figures, ΔI and ΔF traces are shown in black and red, respectively, and bars denote periods of agonist application. Sample recordings for MTS-TAMRA-labeled A52C GlyRs (A), MTS-TAMRA-labeled H201C GlyRs (B) and TMRM-labeled E217C GlyRs (C) are shown in response to saturating (3 mM) glycine and 30 μM ivermectin.

Fig. 2. **Examples of glycine- and ivermectin-mediated ΔF_{max} responses from MTS-TAMRA-labeled Q67C-containing GlyRs.**

A, B and C show examples of glycine- and ivermectin-mediated ΔF_{max} responses from MTS-TAMRA-labeled Q67C, Q67C-A288G and Q67C-A288G-L233W GlyRs, respectively. Agonist applications were made at 3 min intervals.

Fig. 3. **Comparison of glycine- and ivermectin-mediated ΔI_{max} and ΔF_{max} values at MTS-TAMRA-labeled Q67C-containing GlyRs.**

'Glycine1' denotes the first glycine application and 'glycine2' denotes the second. (A) Mean ΔI_{max} and ΔF_{max} values for the labeled Q67C GlyR were normalized to one, with the same normalization factors applied to responses induced by ivermectin and glycine2. In this and subsequent panels, statistical significance is shown relative to glycine1 values. (B, C) Mean ΔI_{max} and ΔF_{max} values for the labeled Q67C-A288G and Q67C-A288G-L233W GlyRs, normalized as in (A). * $P < 0.05$, ** $P < 0.01$ and *** $P < 0.001$ by unpaired t-test.

Fig. 4. **Examples of glycine- and ivermectin-mediated ΔF_{max} responses from AF546-labeled V178C-containing GlyRs.**

A, B and C show examples of glycine- and ivermectin-mediated ΔF_{max} responses from AF546-labeled V178C, V178C-A288G and V178C-A288G-L233W GlyRs, respectively. Agonist applications were made at 3 min intervals.

Fig. 5. **Comparison of glycine- and ivermectin-mediated ΔI_{max} and ΔF_{max} values at AF546-labeled V178C-containing GlyRs.**

'Glycine1' denotes the first glycine application and 'glycine2' denotes the second. (A) Mean ΔI_{max} and ΔF_{max} values for the labeled V178C GlyR were normalized to one, with the same normalization factors applied to responses induced by ivermectin and glycine2. In this and subsequent panels, statistical significance is shown relative to glycine1 values. (B, C) Mean ΔI_{max} and ΔF_{max} values for the labeled V178C-A288G and V178C-A288G-L233W GlyRs, normalized as in (A). * $P < 0.05$, ** $P < 0.01$ and *** $P < 0.001$ by unpaired t-test.

Fig. 6. **Examples of glycine- and ivermectin-mediated ΔF_{max} responses from MTS-TAMRA-labeled N203C-containing GlyRs.**

A, B and C show examples of glycine- and ivermectin-mediated ΔF_{max} responses from MTS-TAMRA-labeled N203C, N203C-A288G and N203C-A288G-L233W mutant GlyRs, respectively. Agonist applications were made at 3 min intervals.

Fig. 7. **Comparison of glycine- and ivermectin-mediated ΔI_{max} and ΔF_{max} values at MTS-TAMRA-labeled N203C-containing GlyRs.**

'Glycine1' denotes the first glycine application and 'glycine2' denotes the second. (A) Mean ΔI_{max} and ΔF_{max} values for the labeled N203C GlyR were normalized to one, with the same normalization factors applied to responses induced by ivermectin and glycine2. In this and subsequent panels, statistical significance is shown relative to glycine1 values. (B, C) Mean ΔI_{max} and ΔF_{max} values for

the labeled N203C-A288G and N203C-A288G-L233W GlyRs, normalized as in (A). * $P < 0.05$, ** $P < 0.01$ and *** $P < 0.001$ by unpaired t-test.

Highlights: (3-5 bullet points. Maximum 85 characters per bullet point including spaces).

- Agonist-induced conformational changes initiate Cys-loop receptor activation
- It is difficult to define which conformational changes are critical for activation
- Ivermectin activates glycine receptors by binding in the transmembrane domain
- We find ivermectin induces conformational changes in 3 glycine-binding domains
- This suggests an allosteric linkage between these domains and the gate

Figure 1

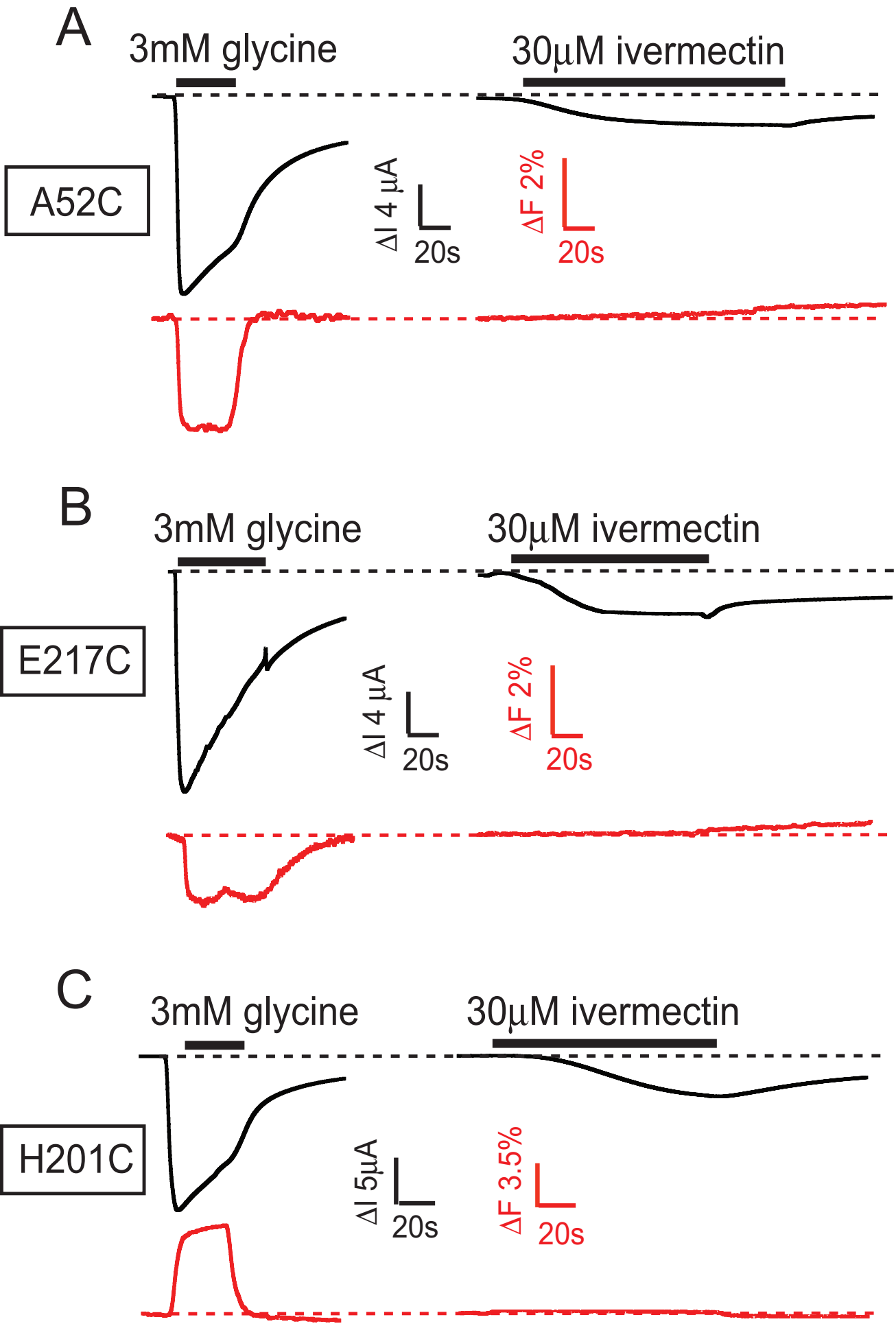
A
3mM glycine
30µM ivermectin
A52C
ΔI 4 µA
20s
ΔF 2%
20s
B
3mM glycine
30µM ivermectin
E217C
ΔI 4 µA
20s
ΔF 2%
20s
C
3mM glycine
30µM ivermectin
H201C
ΔI 5µA
20s
ΔF 3.5%
20s

Figure 2

Click here to download high resolution image

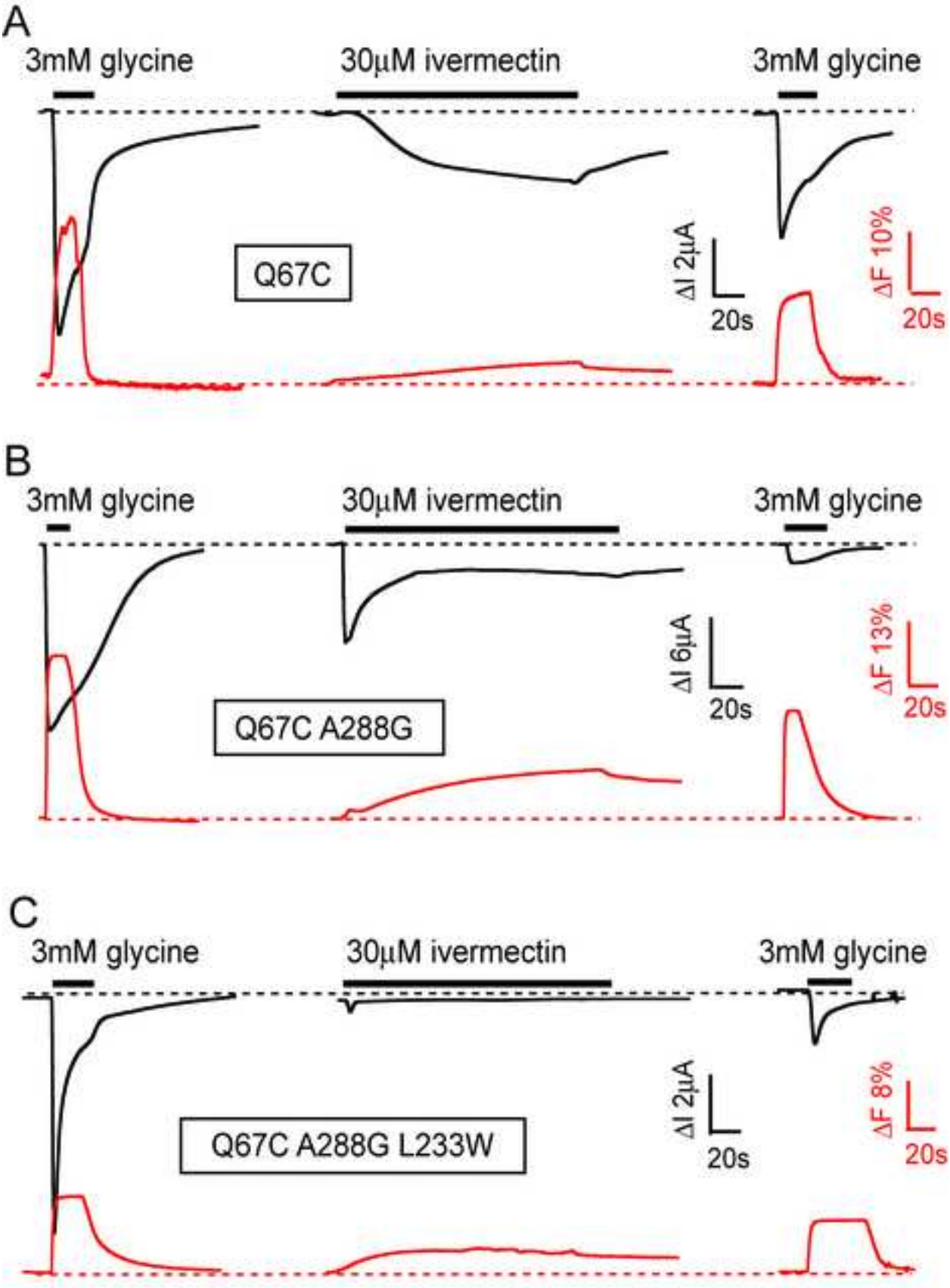

Figure 2

Figure 3

Figure 3

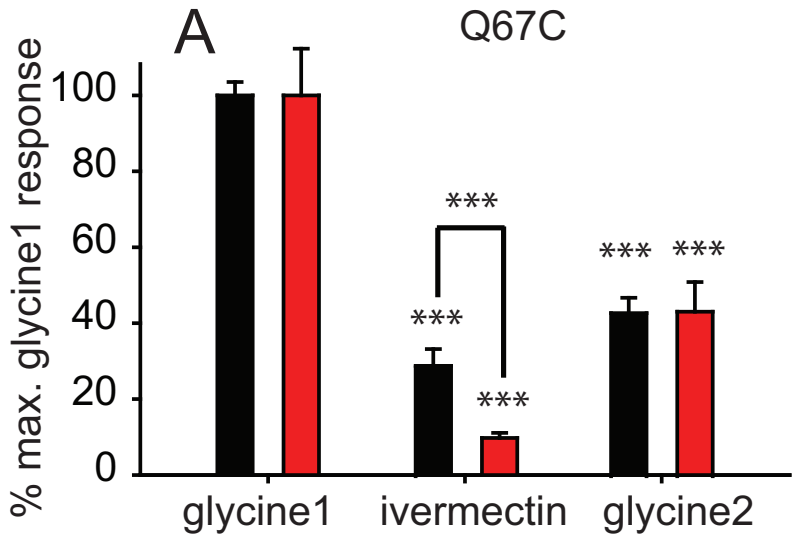

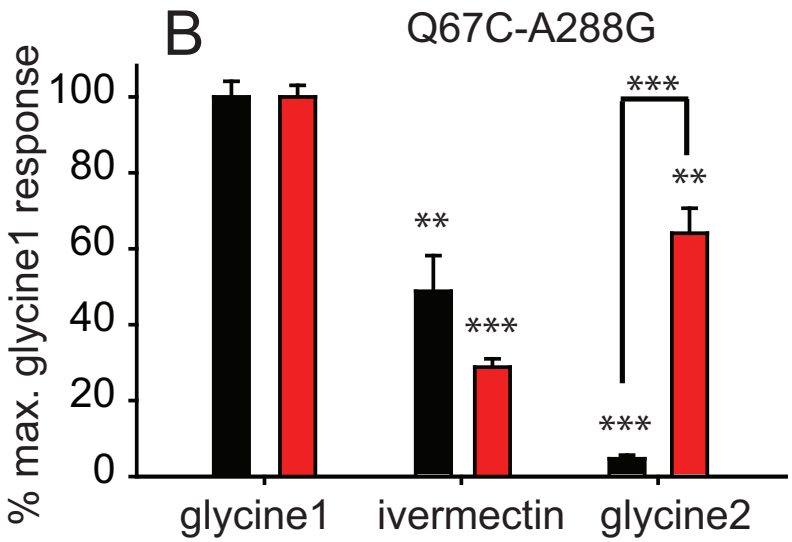

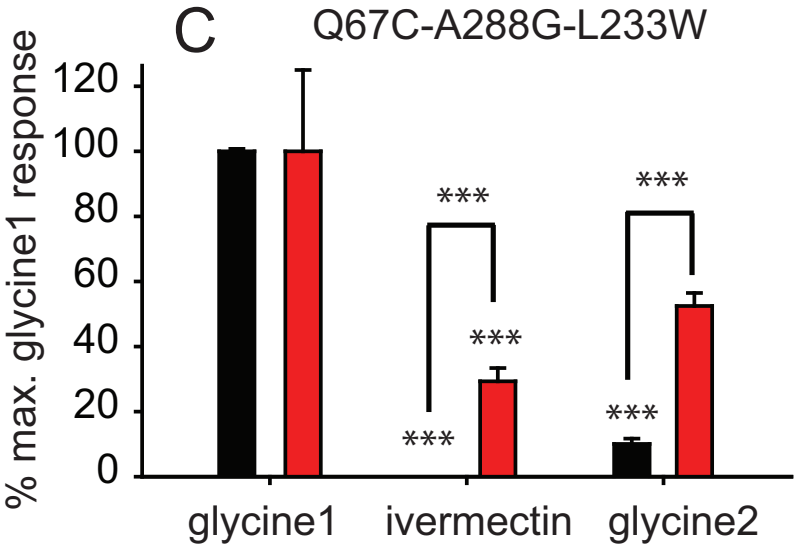

Figure 4

Click here to download high resolution image

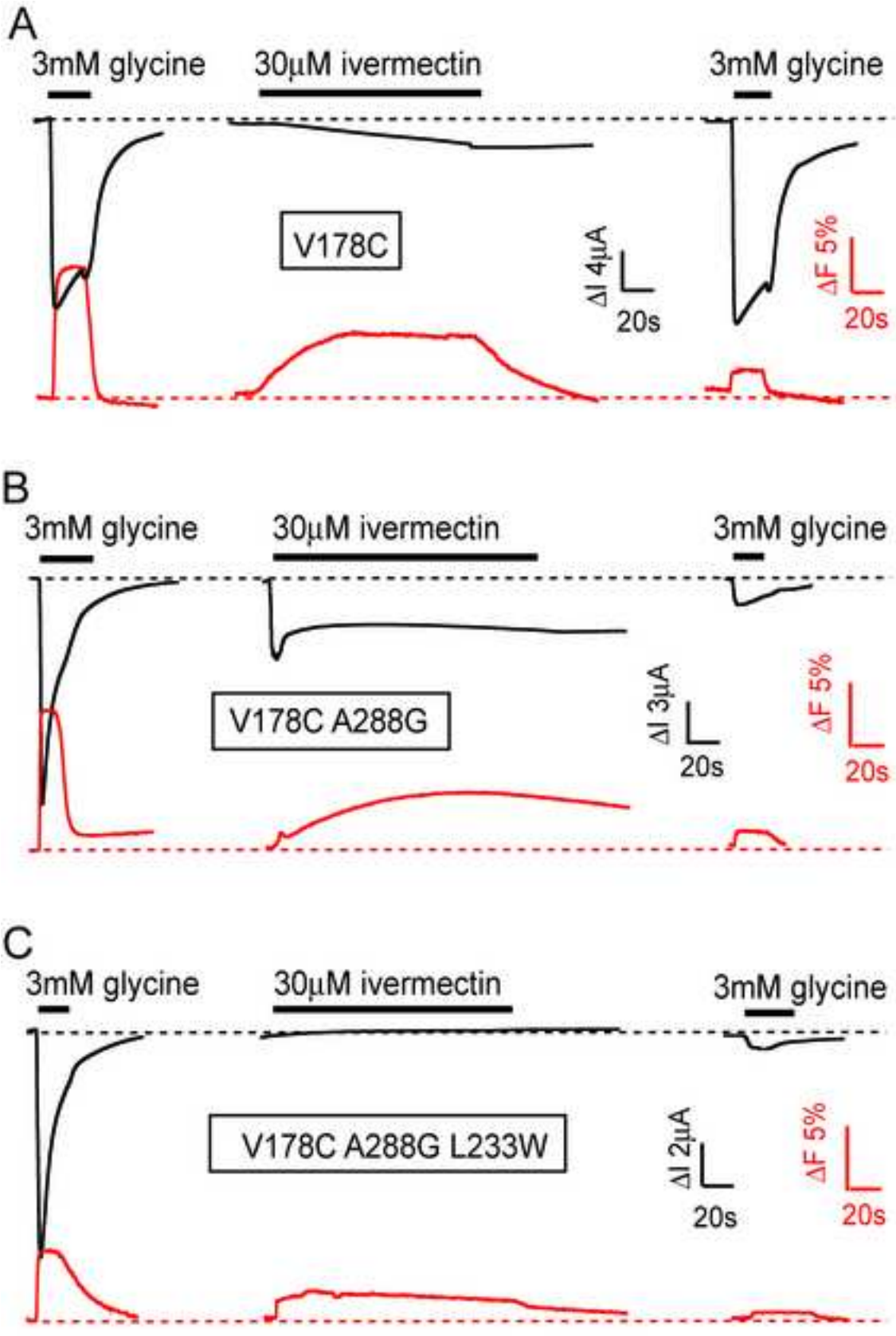

Figure 4

Figure 5

Figure 5

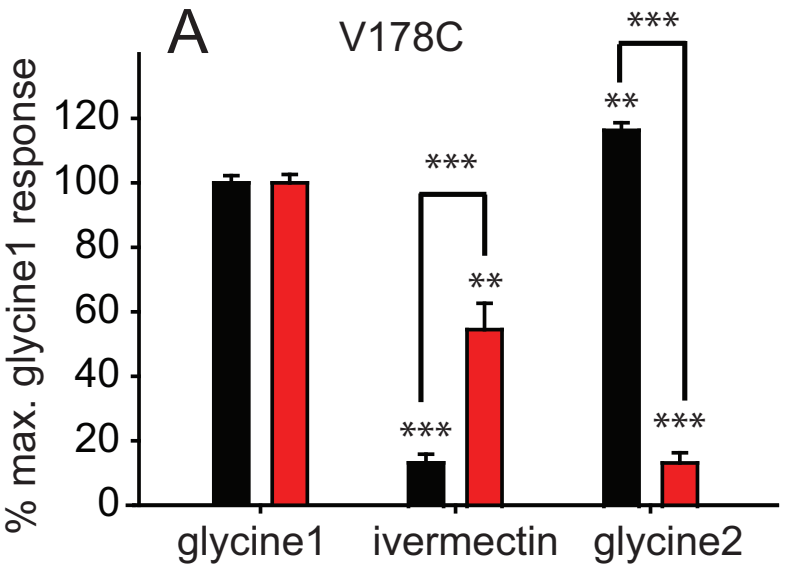

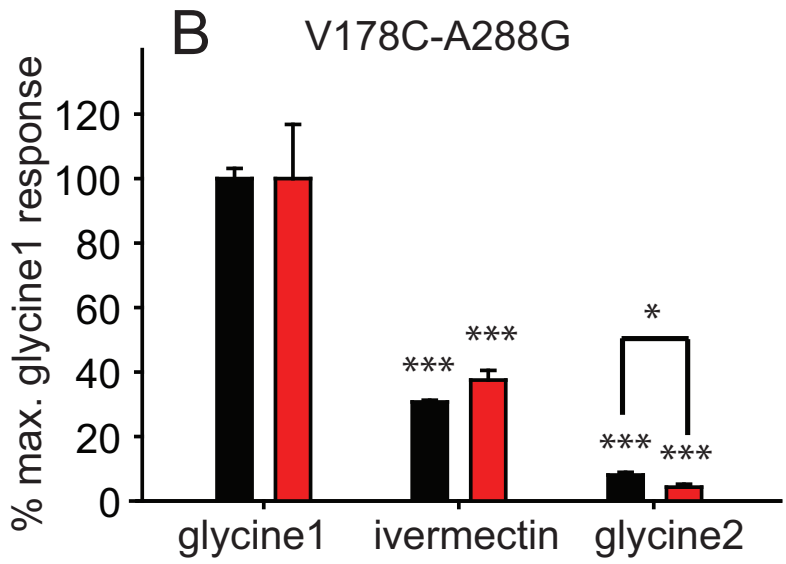

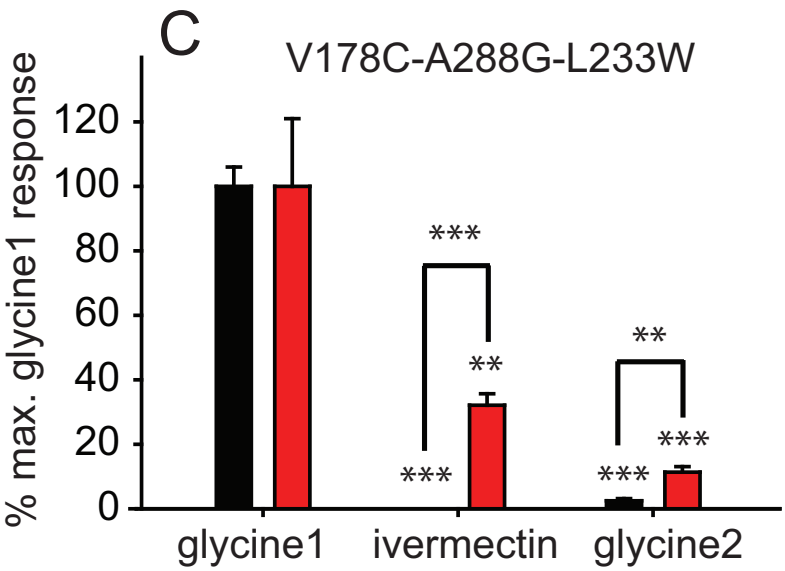

Figure 6

Click here to download high resolution image

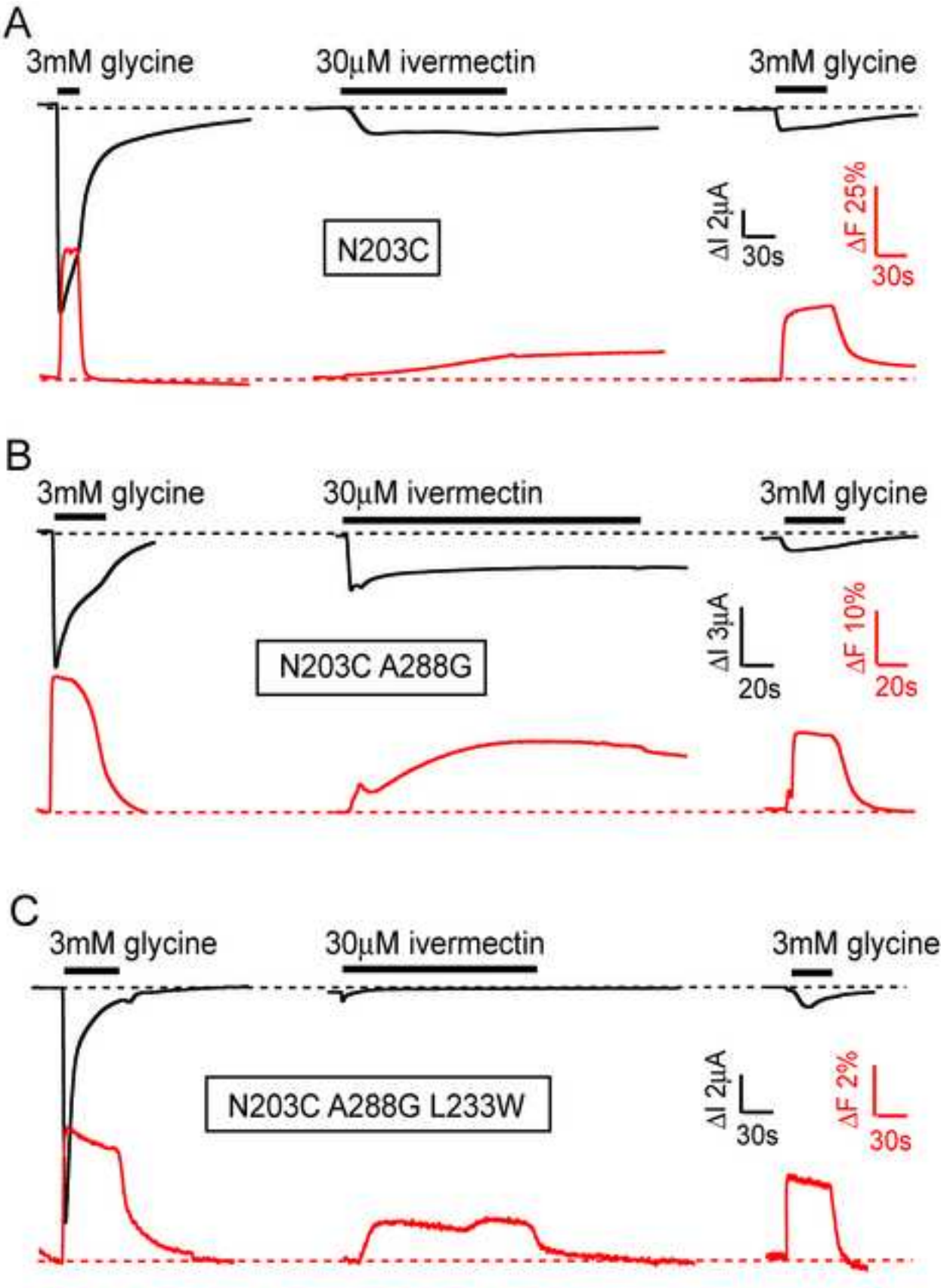

Figure 6

Figure 7

Figure 7

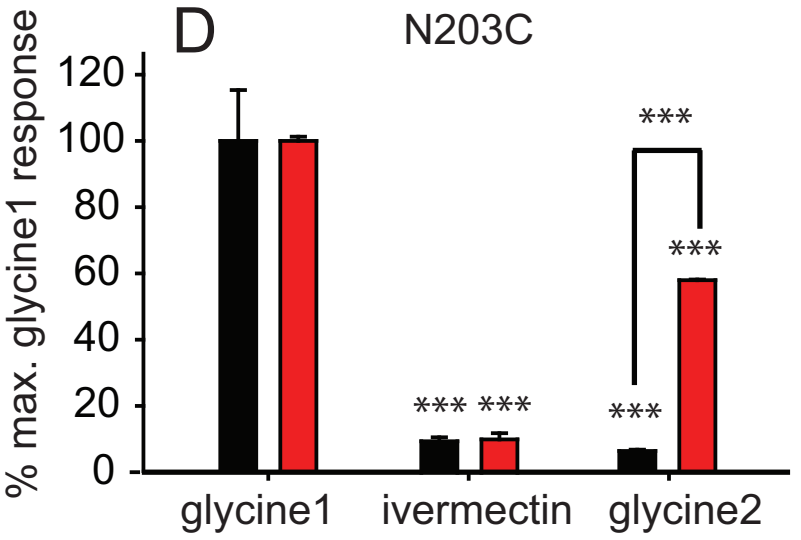

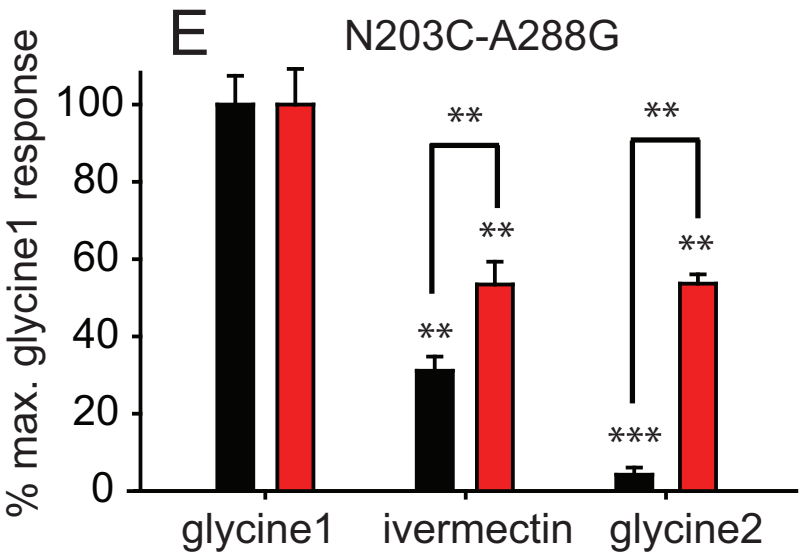

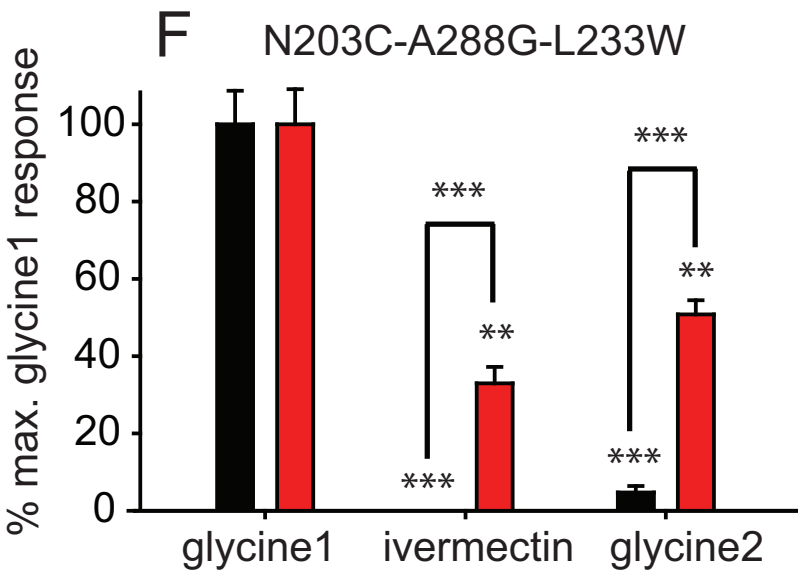

Table 1.

Construct	**EC_{50} (µM)**	**n_H**	**ΔI_{max} (µA)**	**ΔF_{max} (%)**	n
Q67C-A288G α1 GlyR unlabelled	0.6 ± 0.1	3.3 ± 0.2	5.9 ± 0.3	-	4
Q67C-A288G α1 GlyR MTS-TAMRA	2.9 ± 0.5*a*	0.7 ± 0.1*a*	10.4 ± 0.4*a*	-	3
Q67C-A288G α1 GlyR MTS-TAMRA	**281 ± 5*ab***	**2.0 ± 0.1*ab***	**-**	**45 ± 2**	**3**
V178C-A288G α1 GlyR unlabelled	3.8 ± 0.1	1.3 ± 0.1	9.6 ± 0.6	-	3
V178C-A288G α1 GlyR AF546	3.4 ± 0.7	1.1 ± 0.1	10.2 ± 0.5	-	3
V178C-A288G α1 GlyR AF546	**133 ± 17*ab***	**0.8 ± 0.1*ab***	**-**	**19 ± 3**	**3**
N203C-A288G α1 GlyR unlabelled	0.7 ± 0.1	2.8 ± 0.2	7.9 ± 0.5	-	4
N203C-A288G α1 GlyR MTS-TAMRA	0.5 ± 0.1	1.5 ± 0.1*a*	7.5 ± 0.6	-	3
N203C-A288G α1 GlyR MTS-TAMRA	**52 ± 8*ab***	**1.2 ± 0.1*ab***	**-**	**25 ± 3**	**3**

a - significant difference to unlabeled mutant GlyR ($P < 0.05$)

b - significant difference to electrophysiological properties of labeled mutant GlyR ($P < 0.05$)